Synthesis, Crystal Structure, and Ionic Conductivity of Novel Ruddlesden−Popper Related Phases, $Li_4Sr_3Nb_{5.77}Fe_{0.23}O_{19.77}$ and $Li_4Sr_3Nb_6O_{20}$

N. S. P. Bhuvanesh, M. P. Crosnier-Lopez, O. Bohnke, J. Emery,† and J. L. Fourquet*

Laboratoire des Fluorures (UPRES A 6010, CNRS) and Laboratoire de Physique de l'Etat Condensé (UPRES A 6087, CNRS), Faculté des Sciences du Mans, Université du Maine, Avenue O. Messiaen, 72085 Le Mans Cedex 9, France

Received July 20, 1998. Revised Manuscript Received November 12, 1998

We have synthesized two new lithium-containing oxides which are related to Ruddlesden−Popper phases, $Li_4Sr_3Nb_{5.77}Fe_{0.23}O_{19.77}$ and $Li_4Sr_3Nb_6O_{20}$, with partial occupancy of the 12-coordinated sites by Sr, for the first time by direct solid-state reaction. While the single crystal and powder X-ray diffraction data indicate that these oxides crystallize in tetragonal cells (space group $I4/mmm$; $a = 3.9585(2)$ Å, $c = 25.915(3)$ Å and $a = 3.953(2)$ Å, $c = 26.041(5)$ Å for the respective oxides), the electron diffraction of some of the crystallites shows supercell reflections with $a \approx \sqrt{2}a_p$, $c \approx 25.9$ Å, probably indicating a twisting of the NbO_6 octahedra in the *ab*-plane. Although, these oxides show no significant lithium ionic conduction at room temperature, they show distinct conductivity values at elevated temperatures.

Introduction

Perovskites form an important class of materials[1] which, besides forming a large number of stoichiometric oxides, show interesting variations that could be considered as formed with ordered defects of the parent structure.[2] Some of these defect oxides, for instance, the Ruddlesden−Popper (RP)-,[3] Dion−Jacobson (DJ),[4] and the Aurivillius phases,[5] possess perovskite slabs of composition $[A_{n-1}M_nO_{3n+1}]$. RP and DJ phases, having respectively the general formula $A'_2[A_{n-1}M_nO_{3n+1}]$ and $A'[A_{n-1}M_nO_{3n+1}]$ (A' = alkali metal, A = Ca, Ba, La, etc.), are of great interest for many of the properties they exhibit, such as ion-exchange and intercalation,[4,6] ionic conductivity,[7] and photocatalysis.[8] The structure of these compounds could be considered[9] as derived from the perovskite structure with excess A' atoms and oxygen inbetween the MO_6 perovskite layers forming planar defects; removal of TiO_6 octahedral sheets along (0 0 1) followed by a shear of $^1/_2$ [1 1 1] of the remaining perovskite layers defines the planar defect. A related layered defect perovskite oxide of importance, viz., brownmillerite[10] (e.g., Ca_2FeAlO_5), forms with ordered oxygen vacancies along [1 1 0] of perovskite, resulting in alternate octahedra and tetrahedra along the *c*-direction.[10,11]

Other kinds of perovskites of recent interest are the A-site deficient tetragonal $La_{2/3-x}Li_{3x}TiO_3$,[12] and $La_{1/3-x}Li_{3x}MO_3$ (M = Nb, Ta)[13] and the cubic $Li_{2x}Sr_{1-2x}M_{0.5-x}Ta_{0.5+x}O_3$ (M = Cr, Fe, Co, Al, Ga, In, Y)[14] showing high lithium ion conductivity; values of 3×10^{-4} S cm^{-1} (for $x = 0.10$), $(3-7) \times 10^{-5}$ S cm^{-1} and 1×10^{-4} S cm^{-1} (for M = Fe and $x = 0.25$) have been reported for respective materials. Recently,[15] we have

* To whom correspondence should be addressed.
† Laboratoire de Physique de l'Etat Condensé (UPRES A 6087, CNRS).

(1) (a) Sleight, A. W. *Science* **1988**, *242*, 1519. (b) Cava, R. J. *Science* **1990**, *247*, 656. (c) Goodenough, J. B.; Longo, J. M. *Landoldt-Börnstein Numerical Data and Functional Relationships in Science and Technology*; *New Series, Group III;* Hellwege, K. H., Ed.; Springer-Verlag: Berlin, 1970; Vol. 4a.

(2) Tilley, R. J. D. In *Chemical Physics of Solids and Their Surfaces*; Roberts, M. W., Thomas, J. M., Eds.; The Chemical Society: London, 1980; Vol. 8.

(3) (a) Ruddlesden, S. N.; Popper, P. *Acta Crystallogr.* **1957**, *10*, 538; **1958**, *11*, 54. (b) Armstrong, A. R.; Anderson, P. A. *Inorg. Chem.* **1994**, *33*, 4366. (c) Wright, A. J.; Greaves, C. *J. Mater. Chem.* **1996**, *6*, 1823.

(4) (a) Dion, M.; Ganne, M.; Tournoux, M. *Mater. Res. Bull.* **1981**, *16*, 1429. (b) Dion, M.; Ganne, M.; Tournoux, M. *Rev. Chim. Miner.* **1986**, *23*, 61. (c) Jacobson, A. J.; Johnson, J. W.; Lewandowski, J. T. *Inorg. Chem.* **1985**, *24*, 3727. (d) Gopalakrishnan, J.; Bhat, V.; Raveau, B. *Mater. Res. Bull.* **1987**, *22*, 413. (e) Subramanian, M. A.; Gopalakrishnan, J.; Sleight, A. W.; *Mater. Res. Bull.* **1988**, *23*, 837. (f) Mohan Ram, R. A.; Clearfield, A. *J. Solid State Chem.* **1991**, *94*, 45.

(5) Aurivillius, B. *Ark. Kemi* **1949**, *1*, 463, 499; **1950**, *2*, 519.

(6) (a) Jacobson, A. J.; Lewandowski, J. T.; Johnson, J. W. *J. Less-Common Metals* **1984**, *21*, 92. (b) Jacobson, A. J.; Johnson, J. W.; Lewandowski, J. T. *Mater. Res. Bull.* **1987**, *22*, 45. (c) Gopalakrishnan, J.; Bhat, V. *Inorg. Chem.* **1987**, *26*, 4299.

(7) (a) Park, K.; Byeon, S.-H. *Bull. Korean Chem. Soc.* **1996**, *17*, 168. (b) Toda, K.; Kameo, Y.; Fujimoto, M.; *J. Ceram. Soc. Jpn. Int. Edn.* **1994**, *102*, 735.

(8) (a) Domen, K.; Yoshimura, J. Sekine, T.; Tanaka, A.; Onishi, T. *Catal. Lett.* **1990**, *4*, 339. (b) Ikeda, S.; Tanaka, A.; Hara, M.; Kondo, J. N.; Maruya, K.; Domen, K. *Microporous Mater.* **1997**, *9*, 253. (c) Ikeda, S.; Hara, M.; Kondo, J. N.; Domen, K.; Takahashi, H.; Okubo, T.; Kakihana, M. *Chem. Mater.* **1998**, *10*, 72.

(9) McCoy, M. A.; Grimes, R. W.; Lee, W. E. *Philos. Mag.* A **1997**, *75*, 833.

(10) Colville, A. A.; Geller, S. *Acta Crystallogr. Sect B* **1971**, *27*, 2311.

(11) Uma, S.; Gopalakrishnan, J. *Chem. Mater.* **1994**, *6*, 907.

(12) (a) Inaguma, Y.; Liquan, C.; Itoh, M.; Nakamura, T.; Uchida, T.; Ikuta, H.; Wakihara, M. *Solid State Commun.* **1993**, *86*, 689. (b) Kawai, H.; Kuwano, J. *J. Electrochem. Soc.* **1994**, *141*, L78. (c) Varez, A. Garcia-Alvarado, F.; Moran, E.; Alario-Franco, M. A. *J. Solid State Chem.* **1995**, *118*, 78. (d) Fourquet, J. L.; Duroy, H.; Crosnier-Lopez, M. P. *J. Solid State Chem.* **1996**, *127*, 283. (e) Bohnke, O.; Bohnke, C.; Fourquet, J. L. *Solid State Ionics* **1996**, *91*, 21.

(13) Mizumoto, K.; Hayashi, S. *J. Ceram. Soc. Jpn.* **1997**, *105*, 713.

(14) Watanabe, H.; Kuwano, J. *J. Power Sources* **1997**, *68*, 421.

10.1021/cm980736j CCC: $18.00
Published on Web 02/12/1999

reported proton-exchange in $La_{2/3-x}Li_{3x}TiO_3$ resulting in novel metastable $La_{2/3-x}TiO_{3-3x}(OH)_{3x}$, which on further dehydration yields $La_{2/3-x}TiO_{3-3x/2}$. We have also shown, from our results from impedance spectroscopic analysis and ^1H NMR experiments, that while the protonated phases show no proton mobility, the latter perovskites with oxygen deficiency show distinct oxygen ion conduction. Also, a study of dc conductivity from impedance spectroscopic analysis and ^7Li nuclear magnetic resonance (NMR) spin−lattice relaxation time (T_1) measurements as a function of temperature, to understand the mechanism of conduction in the parent $La_{2/3-x}Li_{3x}TiO_3$,[16] show the presence of two kinds of Li^+ ions in different environments. Moreover, it has been found that the motion of the mobile lithium ions could be correlated or that there is a distribution of activation energy for the Li^+ ion hops which are thermally activated. To understand further the mechanism of Li^+ ion conduction and to study the ion exchange behavior, we were interested in related phases $Li_{2x}Sr_{1-2x}M_{0.5-x}Ta_{0.5+x}O_3$ (for M = Fe), reported by Watanabe and Kuwano,[14] prepared by heating corresponding oxides and carbonates at 1350 °C. We expected that these oxides could possibly yield new protonated and oxygen deficient perovskites, and further, an investigation of ^7Li NMR and ionic conductivity as a function of temperature would throw some light on the mechanism of lithium ion conduction in the three-dimensional perovskites. Our efforts to synthesize these parent materials were not successful under the experimental conditions we employed.[17] But, in the process, working with analogous compounds of Nb in place of Ta, we found single crystals of composition $Li_4Sr_3Nb_{5.77}Fe_{0.23}O_{19.77}$ and $Li_4Sr_3Nb_6O_{20}$ which are related to the RP phases. Here, we report the synthesis, crystal structure, and ionic conductivity of these two title compounds. To our knowledge this is the first report of a lithium-containing RP-related phase, prepared in bulk,[18] by direct solid-state reaction.

Experimental Section

Synthesis of Title Compounds. Single crystals of $Li_4Sr_3Nb_{5.77}Fe_{0.23}O_{19.77}$ were obtained by heating Li_2CO_3 (99.997%), $SrCO_3$ (99%), Nb_2O_5 (99.9%), and Fe_2O_3 (99%), in the molar ratio 0.35:0.30:0.425:0.075, first at 850 °C for 6 h and then at 1050 °C for 12 h, and by allowing the mixture to cool naturally. Then a final heating was given at 1200 °C for 12 h followed by cooling at 2 °C/min down to 200 °C. Several thin transparent single crystals with a pale brown color were selected for further investigations. Single crystals of $Li_4Sr_3Nb_6O_{20}$ were obtained as colorless thin plates by treating a mixture of Li_2CO_3, $SrCO_3$, and Nb_2O_5 in the molar proportion 1.25:1.75:2 at 550 °C for 12 h and at 1200 °C for 24 h followed by natural cooling. After several experiments of trial and error to fix the conditions of temperature and time, which are very critical, we could also prepare the bulk samples of $Li_4Sr_3Nb_{5.77}Fe_{0.23}O_{19.77}$ and $Li_4Sr_3Nb_6O_{20}$ by heating stoichiometric amounts (an excess 10 mol % of Li_2CO_3 was taken to compensate for volatilization at high temperature) of the component oxides and carbonates at 550 °C for 12 h and then at 1050 °C for 6 h.

Table 1. Selected Crystallographic Parameters and Operating Conditions for the X-ray Data Collection and Refinement

	$Li_4Sr_3Nb_{5.77}Fe_{0.23}O_{19.77}$	$Li_4Sr_3Nb_6O_{20}$
symmetry	tetragonal	
space group	*I*4/*mmm*	
$a = b$ (Å)	3.9585(2)	3.953(2)
c (Å)	25.915(4)	26.041(5)
V (Å^3)	406.08	406.93
Z	1	
formula weight	1155.85	1168.05
D_{calc} (g/cm^3)	4.72	4.76
temperature (°C)	20	
radiation	MoKα	
crystal volume ($\times 10^{-4}$ mm^3)	18.3	6.6
scanning mode	$\omega/2\theta$	
aperture (mm)	4 × 4	
range registered:		
2θ max (deg)	100	90
hkl max	8, 6, 55	7, 4, 51
absorption coefficient (cm^{-1})	168.6	114.80
absorption correction	Gaussian	
transmission factors:		
T_{max}, T_{min}	0.107, 0.529	0.203, 0.648
R_{int}	0.0180	0.0326
secondary extinction coefficient	0.012(1)	−
reflections measured total	1482 (114 standards)	1148 (93 standards)
used in refinements	562	392
number of refined parameters	27	26
weighting scheme	w = $1/[\sigma^2(F_o)^2+(AP)^2+(BP)]$, where P = $[\mathrm{Max}(F_o^2,0) + 2F_c^2]/3$	
	$A = 0.1258$	$A = 0.1784$
	$B = 22.02$	$B = 0.0$
electron density in final Fourier difference map: max, min (e$^-$/Å^3)	2.15, −2.77	2.65, −2.23
R_1 (for $F_o > 4\sigma(F_o)$) and for all data	0.0263, 0.0377	0.0312, 0.0602

Single-Crystal Analysis. The single crystals of the compounds were first analyzed by standard precession X-ray photographic methods. The analysis suggested a tetragonal symmetry (~3.9 Å, 25.9 Å) with 4/*mmm* Laue class and the systematic absences leading to an extinction symbol I - - -, with possible space groups *I*422 (No. 97), *I*4*mm* (No. 107), I$\bar{4}$*m*2 (No. 119), I$\bar{4}$2*m* (No. 121), and *I*4/*mmm* (No. 139).

The experimental condition for the collection of XRD data on a Siemens AED2 four-circle diffractometer are listed in Table 1. The lattice parameters were refined by the double scan technique from the position of 28 reflections in the vicinity of 30° (2θ). Four-circle single-crystal diffractometer data were analyzed with the SHELX-93 program[19] and atomic scattering factors, $\Delta f'$ and $\Delta f''$ of Li^+, Sr^{2+}, and Nb^{5+} and Fe^{3+} ions, were taken from *International Tables of Crystallography*.[20] For O^{2-}, the above values were taken from ref 21.

(15) Bhuvanesh, N. S. P.; Bohnke, O.; Duroy, H.; Crosnier-Lopez, M. P.; Emery, J.; Fourquet, J. L. *Mater. Res. Bull.* **1998**, *33*, 1681.

(16) Bohnke, O.; Emery, J.; Veron, A.; Fourquet, J. L.; Buzare, J. Y.; Florian, P.; Massiot, D. *Solid State Ionics* **1998**, *109*, 25.

(17) Stoichiometric quantities of Li_2CO_3, $SrCO_3$, Ta_2O_5, and Fe_2O_3 corresponding to the composition $Li_{2x}Sr_{1-2x}Fe_{0.5-x}Ta_{0.5+x}O_3$, for various values of *x*, were heated in platinum crucibles, first at 850 °C for 12 h, followed by heating at 1300 °C for 1 h, and allowed to cool naturally.

(18) Recently, single crystals of $Li_2La_{0.833}(Nb_{1.5}Ti_{0.5})O_7$ and $Li_2La_{2.25}(Nb_{1.25}Ti_{2.75})O_{13}$ related to RP phases has been obtained by direct solid-state reaction, along with other products such as $LaTiNbO_6$ and $LaNbO_4$, in our laboratory (Crosnier-Lopez, M. P.; Duroy, H.; Fourquet, J. L. *Mater. Res. Bull.* In press). We believe the present work is the first reported synthesis of lithium-containing RP phase in bulk and single crystals by this reaction route.

(19) Sheldrick, G. M.; *Shelx-93: A Program for the Refinement of Crystal Structures from Diffraction Data*; University of Göttingen, Germany, 1993.

(20) *International Tables for X-ray Crystallography*; Kynoch Press: Birmingham, 1974; Vol. IV.

(21) Suzuki, T. *Acta Crystallogr.* **1960**, *13*, 279.

Table 2. Fractional Atomic Coordinates, Anisotropic Thermal Parameters U_{ij} (Å^2 × 10^4), and Isotropic Thermal Parameter U_{eq} for $Li_4Sr_3Nb_{5.77}Fe_{0.23}O_{19.77}$[a]

atom	site	*x*	*y*	*z*	sof	U_{11}	U_{22}	U_{33}	U_{23}	U_{13}	U_{12}	U_{eq}
Sr	4e	0.5	0.5	0.07906(2)	0.0942(5)	76(1)	76(1)	95(2)	0	0	0	82(1)
				0.07907(2)	*0.0942(4)*	*76(1)*	*76(1)*	*95(1)*				*83(1)*
Nb1	2a	0	0	0	0.0553(8)	73(1)	73(1)	71(2)	0	0	0	72(1)
					0.0549(7)	*71(1)*	*71(1)*	*71(1)*				*71(1)*
Fe1	2a	0	0	0	0.0071(8)	73(1)	73(1)	71(2)	0	0	0	72(1)
					0.0075(7)	*71(1)*	*71(1)*	*71(1)*				*71(1)*
Nb2	4e	0	0	0.15735(2)	0.125	77(1)	77(1)	82(1)	0	0	0	79(1)
				0.15735(1)		*78(1)*	*78(1)*	*81(1)*				*79(1)*
O1	4e	0	0	0.2287(1)	0.125	129(7)	129(7)	84(9)	0	0	0	114(4)
				0.2287(1)		*127(6)*	*127(6)*	*85(8)*				*113(4)*
O2	8g	0	0.5	0.1501(1)	0.25	125(8)	56(6)	231(10)	0	0	0	137(3)
				0.1502(1)		*127(7)*	*56(5)*	*233(9)*				*138(3)*
O3	4e	0	0	0.0754(1)	0.125	257(13)	257(13)	60(10)	0	0	0	191(8)
				0.0754(1)		*263(12)*	*263(12)*	*59(9)*				*195(7)*
O4	4c	0	0.5	0	0.125	996(66)	56(12)	208(17)	0	0	0	420(21)
	8j	*0.060(1)*			(*0.0625*)	*145(18)*	*67(11)*	*214(15)*				142(7)
Li	4 d	0	0.5	0.75	0.125							227(24)
												238(22)

[a] In italics are given the respective parameters for the final structure with the O(4) atoms occupying the 8j sites. The change in the U_{11} values of O4 atoms occupying the 4c and the 8j sites are to be noted.

$Li_4Sr_3Nb_{5.77}Fe_{0.23}O_{19.77}$. A crystal of approximate dimensions 0.038 × 0.190 × 0.304 mm^3 with natural boundary faces ±⟨001⟩, ±⟨100⟩, ±⟨210⟩, and ±⟨010⟩ was selected for the X-ray diffraction (XRD) data collection. We could obtain a good starting model by direct methods in the space group *I*4/*mmm*, which gave us the position of one heavy atom for Nb^{5+}, and subsequent Fourier difference synthesis resulted in two other heavy cations, one Sr^{2+} and one Nb^{5+}, four anionic sites, and finally one position for Li^+ (Table 2). Here we assumed a formula close to $LiSr_2Nb_3O_{10}$, similar to $LiCa_2Ta_3O_{10}$ with the Li atoms having a half-occupancy at the 4d site,[22] and the *R* factor did not decrease below a value of 0.08. Then, on allowing the occupancy of the heavy atoms to be refined, we found the *R* factor decreased rapidly. Analysis of the results indicated that the Sr-4e sites are only partially occupied and gave a formula near to $Li_4Sr_3Nb_6O_{20}$. A quantitative EDX analysis [of Sr, Nb, Fe, and O; JEOL 5800 LV with PGT analyzer (imx pcs)] of the single crystal used for XRD analysis gave us a composition $Li_4Sr_{3.0(3)}Nb_{6.0(3)}Fe_{0.2(1)}O_{20(2)}$ (where the values in parentheses indicate the error in the analysis). Hence, we allowed Fe^{3+} ions to distribute in the Nb^{5+} positions, and we found that Fe^{3+} is statistically distributed at the 2a site, which forms the middle layer of the three-layer-thick MO_6 (M = Nb or Fe) slab (see later). For refinement, the occupancy of the Nb and Fe are tied and also the anisotropic thermal parameters are fixed to be equal. At this stage, we had three possibilities for writing the final formula:

(1) It is possible that we could have excess lithium near the strontium site, in which case the formula could be written as $Li_{4.46}Sr_3Nb_{5.77}Fe_{0.23}O_{20}$, but we could not obtain a single phase product with this latter composition in bulk.

(2) We can have oxygen vacancies associated with Fe^{3+} ions and hence the formula $Li_4Sr_3Nb_{5.77}Fe_{0.23}O_{19.77}$. This kind of vacancies is well-known in layered perovskites of the kind $ACa_2Nb_{3-x}M_xO_{10-x}$ (A = Rb, Cs; M = Al, Fe).[11]

(3) It is also possible that the crystals can have microdomains with different values of *x* in $Li_4Sr_3Nb_{6-x}Fe_xO_{20-x}$, in which case we cannot fix the exact composition.

Since it is difficult to prove the latter possibility, we write the final formula of the compound as $Li_4Sr_3Nb_{5.77}Fe_{0.23}O_{19.77}$, where we assume the presence of oxygen vacancies. This formulation is supported from our experiments by preparation of the phase in bulk. A refinement of occupancy of oxygen atoms did not deviate from unity, probably indicating that the oxygen vacancies are disordered in the possible O4 and O3 sites. We list the atomic parameters with the anisotropic thermal parameters in Table 2. Surprisingly, we found the anisotropic thermal parameter, U_{11}, for the O4 atom, occupying the 4c sites, to be abnormally high, which indicated some anomaly in the *x*-direction (Table 2). We tried to substitute these atoms in 8j sites (*x* $^1/_2$ 0), which refined to a very small value of *x* (∼0.06) with half-occupancy, and we found that the U_{11} decreased to a reasonable value (Table 2, given in italics).

With absorption correction, anisotropic thermal parameters (except for Li^+), a weighting scheme, and 27 parameters, the final stage of refinement converged to R = 0.0263 for 562 data with $F_o > 4\sigma(F_o)$ and $R = 0.0377$ for all the 694 data. The final Fourier difference synthesis was featureless, with maxima and minima around ±2.77 e$^-$/Å^3.

$Li_4Sr_3Nb_6O_{20}$. A crystal of approximate size 0.038 × 0.111 × 0.171 mm^3 with the faces ⟨010⟩, ⟨$\bar{1}$20⟩, ⟨$\bar{1}\bar{2}$0⟩, ±⟨001⟩ and ±⟨100⟩ was chosen for data collection. The starting model and further Fourier different synthesis were obtained similar to $Li_4Sr_3Nb_{5.77}Fe_{0.23}O_{19.77}$ described above. We found that the O4 atoms had to be placed in the 8j sites as in the former case to have meaningful values of U_{11} (Table 3). The final refinement, with conditions as before for $Li_4Sr_3Nb_{5.77}Fe_{0.23}O_{19.77}$ (except that, here, we do not have Fe atoms), with 26 parameters, converged to $R = 0.0312$ for 392 data with $F_o > 4\sigma(F_o)$ and $R = 0.0602$ for all the 548 data and a formula near to $Li_4Sr_3Nb_6O_{20}$. The EDX analysis of this phase gave us a composition $Li_4Sr_{2.9(2)}Nb_{6.0(4)}O_{20(2)}$ (where the values in parentheses indicate the error in the analysis), in agreement with our formulation. The final Fourier difference synthesis was featureless, with maxima and minima around ±2.6 e$^-$/Å^3. We give in Table 3 the atomic parameters along with thermal parameters for $Li_4Sr_3Nb_6O_{20}$.

For both the compounds a test with other possible space groups did not improve the results.

Electron Diffraction (ED). The transmission electron microscopy was performed with a JEOL 2010 electron microscope operating at 200 kV equipped with a side-entry ±30° double tilt specimen holder. Crystals of $Li_4Sr_3Nb_{5.77}Fe_{0.23}O_{19.77}$ and $Li_4Sr_3Nb_6O_{20}$ were ground and ultrasonically dispersed in *n*-butanol. Drops of this dispersion were placed on a Cu grid covered with a holey carbon film.

Ionic Conductivity Measurements. The electrical conductivity measurements of $Li_4Sr_3Nb_{5.77}Fe_{0.23}O_{19.77}$ and $Li_4Sr_3Nb_6O_{20}$, prepared in bulk, were carried out on as-prepared pellets of diameter ∼12 mm and thickness ∼3 mm with sputtered gold coated on the surface as electrodes. A Solartron 1260 Impedance Gain Phase Analyzer with the Z60 Impedance Software for data acquisition was used for the impedance spectroscopic analysis in the frequency range from15 MHz to 1 Hz with an applied voltage of 100 or 300 mV (rms). Samples were fixed up in a two-probe cell, and the data were obtained in the temperature range 30−500 °C in a dry nitrogen atmosphere. Samples were allowed to equilibrate for 1 h at

(22) Toda, K.; Sato, M. *J. Mater. Chem.* **1996**, *6*, 1067.

Table 3. Fractional Atomic Coordinates, Anisotropic Thermal Parameters U_{ij} (Å^2 × 10^4), and Isotropic Thermal Parameter U_{eq} for $Li_4Sr_3Nb_6O_{20}$[a]

atom	site	x	y	z	sof	U_{11}	U_{22}	U_{33}	U_{23}	U_{13}	U_{12}	U_{eq}
Sr	4e	0.5	0.5	0.08014(3)	0.0953(7)	76(2)	76(2)	95(3)	0	0	0	83(2)
				0.08014(3)	*0.0955(6)*	*78(2)*	*78(2)*	*95(3)*				*84(2)*
Nb1	2a	0	0	0	0.0625	80(2)	80(2)	87(3)	0	0	0	82(1)
						78(2)	*78(2)*	*87(2)*				*81(1)*
Nb2	4e	0	0	0.15740(2)	0.125	82(2)	82(2)	95(2)	0	0	0	86(1)
				0.15740(2)		*82(2)*	*82(2)*	*94(2)*				*86(1)*
O1	4e	0	0	0.2278(2)	0.125	133(12)	133(12)	82(15)	0	0	0	116(8)
				0.2278(2)		*136(12)*	*136(12)*	*83(14)*				*119(7)*
O2	8g	0	0.5	0.1496(1)	0.25	125(14)	67(12)	216(17)	0	0	0	136(6)
				0.1497(1)		*128(13)*	*68(11)*	*216(16)*				*137(6)*
O3	4e	0	0	0.0745(2)	0.125	215(18)	215(18)	83(18)	0	0	0	171(11)
				0.0745(2)		*223(17)*	*223(17)*	*79(17)*				*175(11)*
O4	4c	0	0.5	0	0.125	1169(96)	51(22)	176(25)	0	0	0	465(30)
	8j	*0.065(1)*			*(0.0625)*	*170(38)*	*67(21)*	*187(23)*				*141(13)*
Li	4d	0	0.5	0.75	0.125							252(36)
												255(34)

[a] In italics are given the respective parameters for the final structure with the O(4) atoms occupying the 8j sites. The change in the U_{11} values of O4 atoms occupying the 4c and the 8j sites are to be noted.

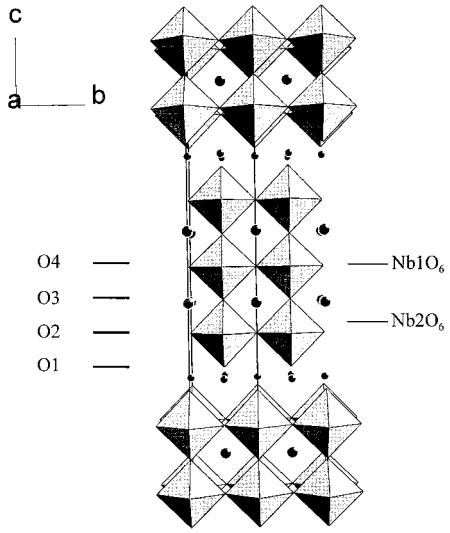

Figure 1. Structure of $n = 3$ RP-related phases, $Li_4Sr_3Nb_{5.77}Fe_{0.23}O_{19.77}$ and $Li_4Sr_3Nb_6O_{20}$. The levels of various oxygen atoms are indicated at the left, small and larger circles represent lithium and strontium ions, respectively.

the temperature of measurement prior to data acquisition in order to obtain reproducible spectra. The temperature was first increased to 500 °C for 1 day and then measurements were performed on cooling followed by a second heating to confirm reproducibility.

Nuclear Magnetic Resonance Analysis. The ^{7}Li NMR spectra were recorded at room temperature with an MSL 300 spectrometer operating at 116.589 MHz with a Bruker 4 mm MAS probe. MAS spectra were obtained at 14 kHz, and a simple sequence (τ − acquisition) with cyclops was used. The processing and acquisition parameters were as follows: 6 μs single $\pi/2$ pulse duration; recycle time, 1 s; spectral width, 125 kHz; time domain, 2 K; 256 scans. Detection was obtained by the cyclop procedure. The ^{7}Li chemical shift are given in parts per million with respect to an external reference of saturated LiCl solution.

Results and Discussion

Structural Description. The analysis of the single-crystal diffraction data of both $Li_4Sr_3Nb_{5.77}Fe_{0.23}O_{19.77}$ and $Li_4Sr_3Nb_6O_{20}$ yields a typical structure as shown in Figure 1. It can be seen that the structure is related to the $n = 3$ RP phases, $A'_2[A_{n-1}M_nO_{3n+1}]$, except for the 12-coordinated A site, which is partially occupied by the Sr atoms. The formula of these phases could also be written as $Li_2Sr_{1.5}Nb_{3-x}Fe_xO_{10-x}$ (for $x = 0.115$ and 0 for the respective phases) in relation to RP phases, $A'_2[A_{n-1}M_nO_{3n+1}]$, with $n = 3$. The structure can be thus described as being formed by cutting the perovskite structure with a slab thickness of three MO_6 (either Nb or Nb/Fe) octahedra, with the alternate layers shifted by $(a + b)/2$ along (0 0 1), similar to $n = 3$ RP phases.

We find the $Nb2O_6$ octahedra, which form the outer layer of the slabs, to be distorted, resulting in four equilateral Nb2−O2 bonds of equal length (∼1.99 Å), a short Nb2−O1 (∼1.85 Å) bond and a long Nb2−O3 (∼2.12 Å) bond (Figure 2, Table 4) caused by the off-centering of the Nb atoms in the NbO_6 octahedra. This distortion, resulting in long and short bonds along the *c*-axis, is well-known in layered perovskites; for example, values such as ∼1.7 and 2.4 Å are reported for the long and the short bonds, respectively.[23] A relatively smaller magnitude of the off-centering in our phases could probably due to the partial occupancy of the strontium atoms. The O4 occupying the 8j site (0.06 $^1/_2$ 0) instead of the 4c sites (0 $^1/_2$ 0) (for the reasons described before) results in twisting of the Nb1/Fe1$(O4)_4$-$(O3)_2$ octahedra in the *ab*-plane and allows the O4 atoms a small displacement. As a consequence, the Nb1/Fe1−O4 bond length increases from ∼1.97 to ∼1.99 Å. This twisting is probably a consequence of the $Nb2O_6$ octahedra in the outer layers forming short bonds (pointing toward lithium ions) and long bonds (pointing toward the middle layer octahedra) and this distortion forcing the Nb1/Fe1O_6 octahedra (in which the Nb1 is a d^0 cation, which prefers to be off-centered[23]) to be twisted. Here, we assume that the four O4 atoms occupy statistically the eight possible (x $^1/_2$ 0) sites. A calculation of the bond valence (Table 5) for $Li_4Sr_3Nb_6O_{20}$ with the O4 atoms in 4c sites and in the 8j sites, favors the latter positions with the average charge on niobium being closer to 5+. If we presume that the O4 atoms are arranged in an ordered fashion (Figure 2b), we should have a larger cell with a dimension of $\sqrt{2}a_p$. However, we observe no weak reflections indicating

(23) (a) Bhuvanesh, N. S. P.; Gopalakrishnan, J. *J. Mater. Chem.* **1997**, *7*, 2297 and the related references therein. (b) Kunz, M.; Brown, I. D. *J. Solid State Chem.* **1995**, *115*, 395.

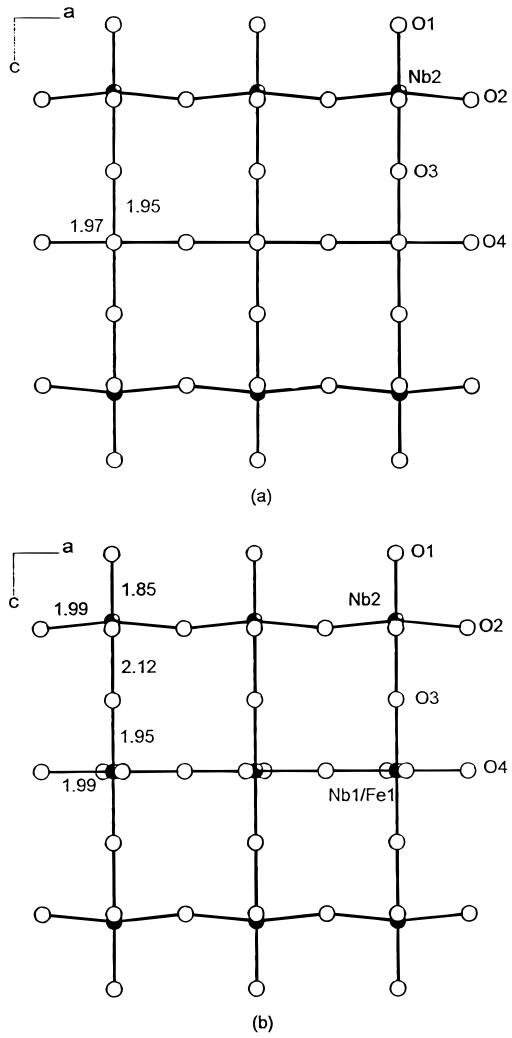

Figure 2. A layer of $Li_4Sr_3Nb_{6-x}Fe_xO_{20-x}$, viewed along *b*, showing the distortions in the NbO_6 octahedra; Li and Sr atoms are not shown. The O4 atoms occupy the 4c sites (0 $^1/_2$ 0) in panel a and with ordered half-occupancy at the 8j sites (0.06 $^1/_2$ 0) in panel b. A twisting of the middle $(Nb1/Fe1)O_6$ octahedra is seen in the latter. In panel a, Nb1 atoms are hidden behind O4 atoms.

formation of such a larger cell in our powder and single-crystal X-ray studies.

The Li atoms are found to interleave the slabs with a distorted tetrahedral coordination with a Li−O distance of ∼2.05 Å. Though, the lithium ions forms two-dimensional sheets in the direction perpendicular to the *c*-axis, the distance between two adjacent $Sr_{1.5}Nb_{3-x}Fe_xO_{10-\delta}$ slabs (∼1.15 Å, obtained by the difference in the *z*-coordinates of the two terminal O1 atoms in the neighboring Sr−Nb−O layers) is small, indicating that $Li_4Sr_3Nb_{5.77}Fe_{0.23}O_{19.77}$ and $Li_4Sr_3Nb_6O_{20}$ could be considered three-dimensional.

We could synthesize $Li_4Sr_3Nb_{5.77}Fe_{0.23}O_{19.77}$ in bulk, the powder X-ray diffraction of which shows (Figure 3a) a very small impurity of $LiNbO_3$, which we were unable to avoid under several conditions tried. On the other hand, we could obtain pure $Li_4Sr_3Nb_6O_{20}$ in bulk (Figure 3b). The preparation of these phases in bulk single phases requires critical conditions, probably because of the formation of intergrowth structures with different slab thickness, as is known in the case of similar RP phases (e.g., SrTiO3−SrO system[9]). Although, there has been a considerable number of reports on the RP phases, the structure of most of them has been obtained by the powder diffraction studies. We believe that this is the

Table 4. Selected Interatomic Distances (Å) and Angles (deg)

$Li_4Sr_3Nb_{5.77}Fe_{0.23}O_{19.77}$

SrO_{12} Polyhedron

4 × Sr−O2	2.705
4 × Sr−O3	2.803
4 × Sr−O4	2.668
⟨Sr−O⟩	2.725

$[Nb1/Fe1]O_6$ Octahedron

Nb1/Fe1	O3	O3	O4	O4	O4	O4
O3	1.955(3)	3.910(4)	2.792(4)	2.792(4)	2.792(2)	2.792(2)
O3	180.0(2)	1.955(3)	2.792(4)	2.792(4)	2.792(2)	2.792(2)
O4	90.0(3)	90.0(3)	1.993(4)	3.958(6)	3.137(4)	2.819(5)
O4	90.0(3)	90.0(3)	166.2(4)	1.993(4)	2.819(4)	2.460(4)
O4	90.0(2)	90.0(2)	103.8(2)	90.0(2)	1.993(0)	3.958(0)
O4	90.0(2)	90.0(2)	90.0(3)	76.2(3)	166.2(0)	1.993(0)
⟨Nb1/Fe1−O⟩	1.980					

$Nb2O_6$ Octahedron

Nb2	O1	O2	O2	O2	O2	O3
O1	1.851(2)	2.840(2)	2.840(2)	2.840(2)	2.840(2)	3.974(4)
O2	95.3(2)	1.988(0)	2.799(0)	3.958(0)	2.799(0)	2.770(2)
O2	95.3(1)	89.5(0)	1.988(2)	2.799(0)	3.958(3)	2.770(3)
O2	95.3(2)	169.3(0)	89.5(0)	1.988(0)	2.799(0)	2.770(2)
O2	95.3(1)	89.5(0)	169.3(2)	89.5(0)	1.988(2)	2.770(3)
O3	180.0(2)	84.7(1)	84.7(2)	84.7(1)	84.7(2)	2.123(3)
⟨Nb2−O⟩	1.987					

LiO_4 Tetrahedron

Li	O1	O1	O1	O1
O1	2.054(0)	3.958(0)	3.007(1)	3.007(1)
O1	149.0(0)	2.054(0)	3.007(1)	3.007(1)
O1	94.1(1)	94.1(1)	2.054(1)	3.958(3)
O1	94.1(1)	94.1(1)	149.0(1)	2.054(0)
⟨Li−O⟩	2.054			

$Li_4Sr_3Nb_6O_{20}$

SrO_{12} Polyhedron

4 × Sr−O2	2.681
4 × Sr−O3	2.799
4 × Sr−O4	2.702
⟨Sr−O⟩	2.727

$Nb1O_6$ Octahedron

Nb1	O3	O3	O4	O4	O4	O4
O3	1.932(5)	3.863(7)	2.778(6)	2.778(6)	2.778(3)	2.778(3)
O3	180.0(4)	1.932(5)	2.778(6)	2.778(6)	2.778(3)	2.778(3)
O4	90.0(5)	90.0(5)	1.996(7)	3.958(10)	3.168(7)	2.823(7)
O4	90.0(5)	90.0(5)	165.0(6)	1.996(7)	2.823(6)	2.429(7)
O4	90.0(3)	90.0(3)	105.0(4)	90.0(4)	1.996(0)	3.958(0)
O4	90.0(3)	90.0(3)	90.0(4)	75.0(4)	165.0(1)	1.996(0)
⟨Nb1−O⟩	1.974					

$Nb2O_6$ Octahedron

Nb2	O1	O2	O2	O2	O2	O3
O1	1.825(5)	2.831(4)	2.831(4)	2.831(4)	2.831(4)	3.972(7)
O2	95.8(3)	1.989(0)	2.799(0)	3.958(0)	2.799(0)	2.777(4)
O2	95.8(2)	89.4(0)	1.989(3)	2.799(0)	3.958(5)	2.777(5)
O2	95.8(3)	168.5(0)	89.4(0)	1.989(0)	2.799(0)	2.777(4)
O2	95.8(2)	89.4(0)	168.5(3)	89.4(0)	1.989(4)	2.777(5)
O3	180.0(4)	84.2(2)	84.2(3)	84.2(2)	84.2(3)	2.147(5)
⟨Nb2−O⟩	1.988					

LiO_4 Tetrahedron

Li	O1	O1	O1	O1
O1	2.061(1)	3.958(0)	3.026(2)	3.026(2)
O1	147.6(1)	2.061(1)	3.026(2)	3.026(2)
O1	94.5(1)	94.5(1)	2.061(2)	3.958(6)
O1	94.5(1)	94.5(1)	147.6(2)	2.061(0)
⟨Li−O⟩	2.061			

Table 5. Values of Bond Valence[a] (s) calculated for $Li_4Sr_3Nb_6O_{20}$[b]

	Sr	Nb1	Nb2	Li	$\sum S$
O1			1.26	0.20	2.06
			(1.23)	(0.20)	(2.03)
O2	0.22		0.81	0.04	2.10
	(0.22)		(0.81)	(0.04)	(2.11)
O3	0.16	0.95	0.53		2.11
	(0.16)	(0.92)	(0.51)		(2.07)
O4	0.21	0.79			2.15
	0.08	(0.84)			(2.19)
	(0.13)				
$\sum$ s	2.07	5.07	5.03	0.89	
	(2.02)	(5.19)	(5.00)	(0.89)	

[a] For the sites i, $S_i = \sum_j[\exp(R_{ij} - d_{ij})/b]$ with $b = 0.37$ and R_{ij} are taken from ref 24. [b] In parentheses are given the values calculated from the positional parameters with the O(4) atoms occupying the 4c sites.

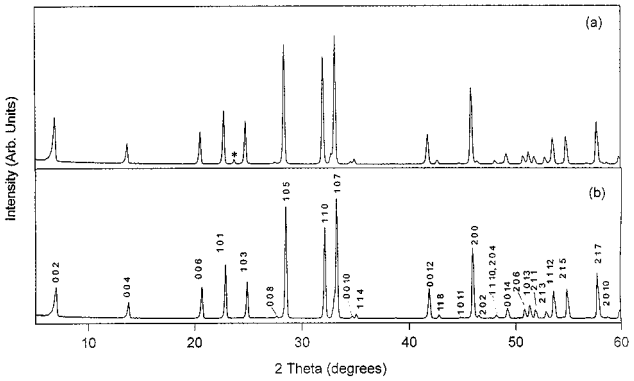

Figure 3. Powder X-ray diffraction patterns (Cu Kα) of (a) $Li_4Sr_3Nb_{5.77}Fe_{0.23}O_{19.77}$ and (b) $Li_4Sr_3Nb_6O_{20}$. In panel a, an asterisk indicates the $LiNbO_3$ impurity.

first report of synthesis of single phase, bulk, and single crystals of Li-containing RP-related phases by direct solid-state reaction.[25]

Electron Diffraction. The electron diffraction of $Li_4Sr_3Nb_{5.77}Fe_{0.23}O_{19.77}$, from several crystallites, and the scan of their reciprocal space show a tetragonal cell ($a \approx a_p$ and $c \approx 25.9$ Å; Figure 4) with body centering. These results are in good agreement with the powder and single-crystal X-ray studies. However, some of the crystallites show diffuse streaks parallel to the c-axis (Figure 5a), indicating disorder along this direction. This could be due to a partial ordering of the O4 atoms (at the 8j) sites in the ab-plane, and the position of the streaks point to a probable tetragonal cell with $a \approx \sqrt{2}a_p$. We could also see distinct weak spots instead of streaks in one of the crystallite (Figure 5b), in [1 $\bar{1}$ 0] ED. This leads to a cell $a \approx \sqrt{2}a_p$, $c \approx 25.9$ Å (Figure 5b,c) (with the condition h 0 l, $l = 2n$, leading to a c-plane), corresponding to a complete ordering of the O4 atoms (Figure 2b). Detailed work is necessary to synthesize and study the exact structural details of the ordered phase.

Ionic Conductivity Measurements and NMR Analysis. From the structure (Figure 1) we see that all the lithium sites are occupied in tetrahedral coordination and there is no room for the mobility of the lithium ions between the $Sr_{1.5}Nb_{3-x}Fe_xO_{10-\delta}$ slabs. Hence, we assumed that there would be no significant conduction in the oxides. Indeed, we observe no measur-

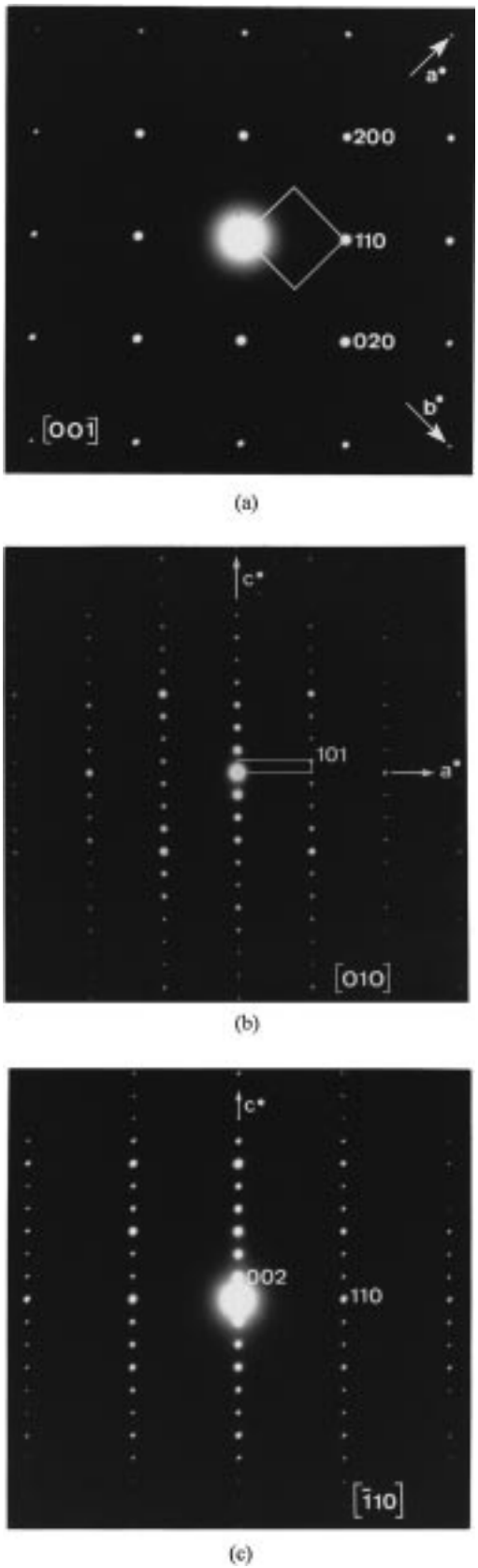

Figure 4. Typical ED patterns of $Li_4Sr_3Nb_{5.77}Fe_{0.23}O_{19.77}$ and $Li_4Sr_3Nb_6O_{20}$ in (a) [0 0 1], (b) [0 1 0], and (c) [$\bar{1}$10] zone axis showing body-centered tetragonal cell.

(24) Brese, N. E.; O'Keeffe, M. *Acta Crystallogr., Sect B* **1991**, *47*, 192.

(25) The syntheses of bulk $Li_2La_2Ti_3O_{10}$, $n = 3$ (Toda, K.; Sato, M. *Mater. Res. Bull.* **1996**, *31*, 1427), by solid-state reaction, and $Li_2LaNb_2O_7$, $n = 2$ (Sato, M.; Jin, T.; Ueda, H. *Chem. Lett.* **1994**, 161), by lithium intercalation, have been reported.

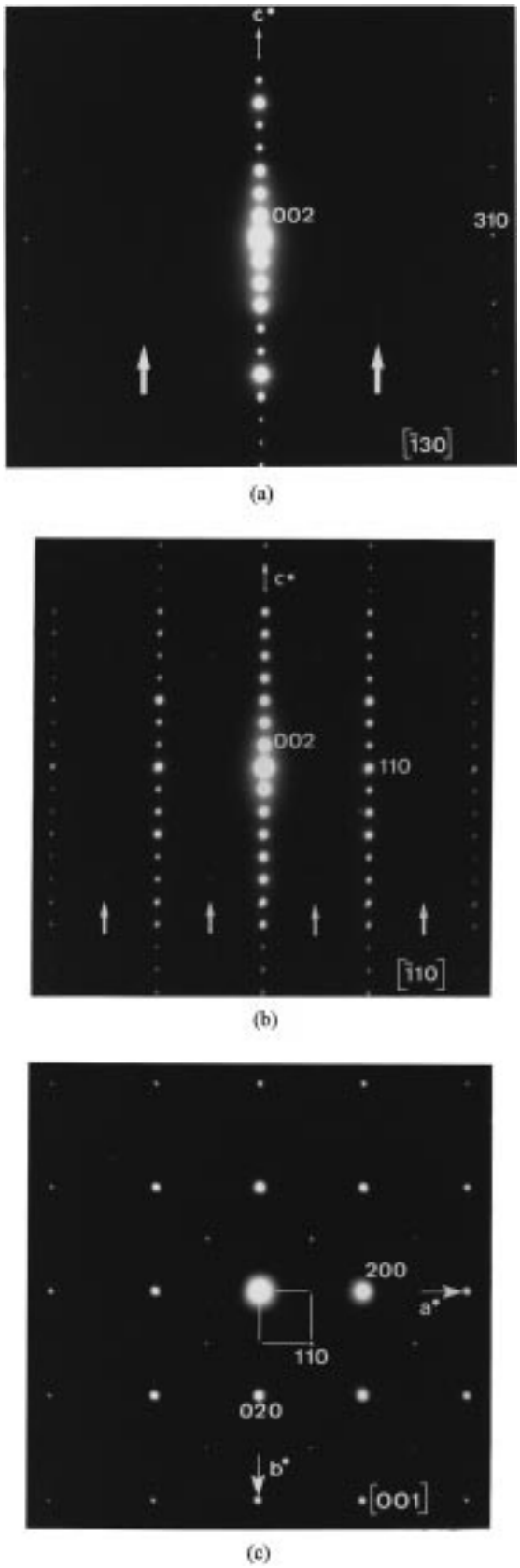

Figure 5. ED patterns showing (a) diffuse streaks ([$\bar{1}$ 3 0] zone axis) and (b) weak spots ([1 1 0] zone axis), indicated by arrows, corresponding to an probable ordering of the O4 atoms. In panel c, the additional spots in the a^*b^* plane which would lead to a larger a parameter are seen.

able lithium ion conduction at room temperature. However with the increasing temperature we observe

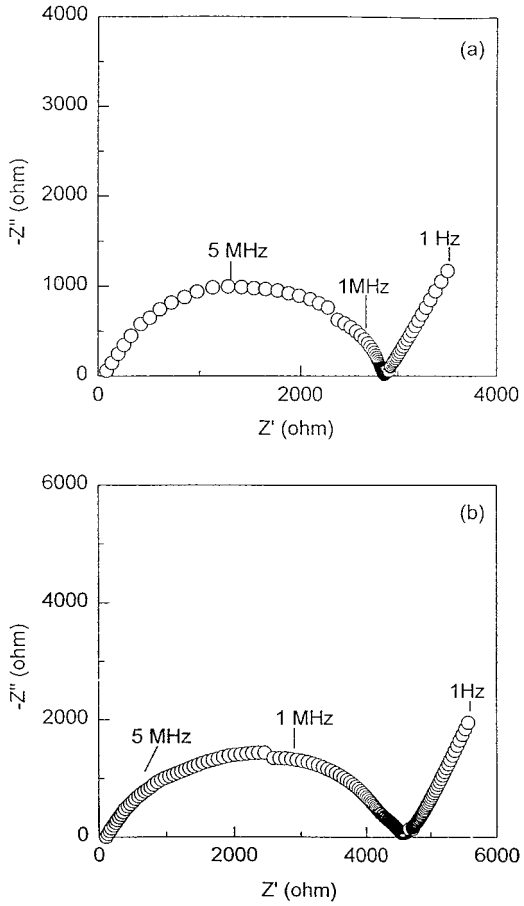

Figure 6. Complex impedance diagrams of (a) $Li_4Sr_3Nb_{5.77}Fe_{0.23}O_{19.77}$ at 375 °C and (b) $Li_4Sr_3Nb_6O_{20}$ at 390 °C.

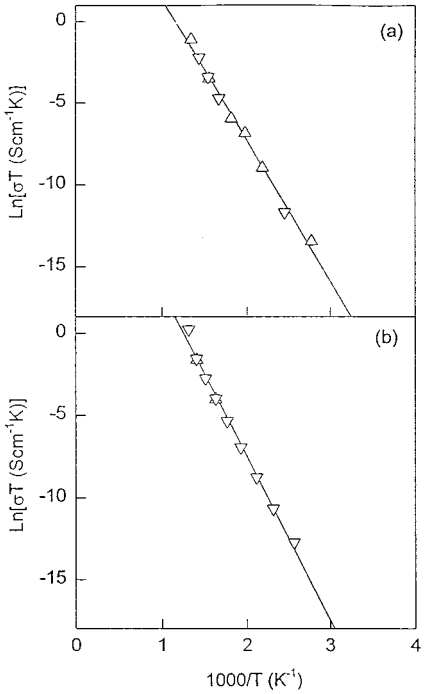

Figure 7. Plot of ln σT as a funtion of $1000/T$ for (a) $Li_4Sr_3Nb_{5.77}Fe_{0.23}O_{19.77}$ and (b) $Li_4Sr_3Nb_6O_{20}$. The downward and upward triangles indicate the measurements made during the cooling and the heating, respectively.

a significant conductivity, 9.6×10^{-5} S cm^{-1} at 390 °C for $Li_4Sr_3Nb_{5.77}Fe_{0.23}O_{19.77}$ and 4.8×10^{-5} S cm^{-1} at 375 °C for $Li_4Sr_3Nb_6O_{20}$ (Figure 6). On plotting ln σT vs

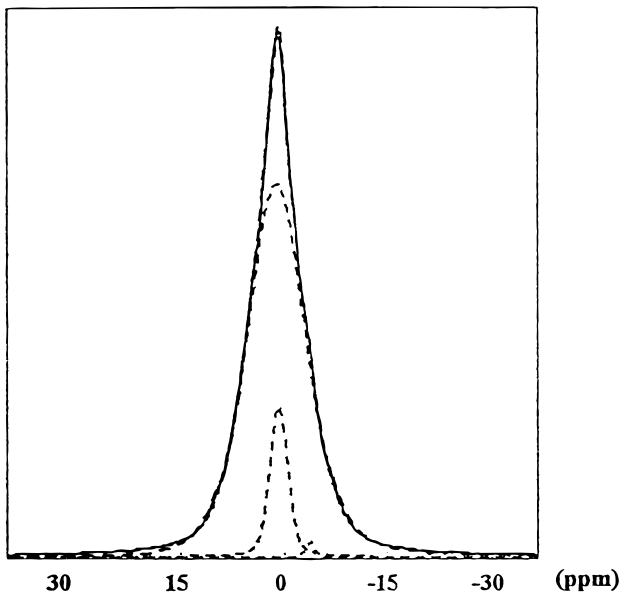

Figure 8. ^{7}Li MAS NMR spectrum of $Li_4Sr_3Nb_6O_{20}$ at room temperature. The solid lines show the observed spectrum and the dotted lines correspond to the peak positions obtained by an extended version of the Bruker Winfit Software.[26]

1000/*T* (Figure 7) we see that the conduction follows an Arrhenius law with an activation energy of 0.88 and 0.74 eV for the respective oxides. The activation energy is much higher as compared to the $La_{2/3-x}Li_{3x}TiO_3$, the three-dimensional perovskites.[11e] We assume that the conduction at elevated temperature is probably due to the lithium ions moving to the vacant Sr sites and hence finding the conduction path. To investigate if we have more than one kind of Li^+ ion, which would let us know the probable path of ionic conduction, we recorded the MAS ^{7}Li NMR of $Li_4Sr_3Nb_6O_{20}$ at room temperature. Using an extended version of Bruker Winfit Software,[26] we could fit the observed MAS spectrum corresponding to three peaks in the proportion 87.3%:12.3%:0.4%, at room temperature. Thus, while our single crystal X-ray diffraction results indicate only one position for the Li ions, the NMR analysis, which probes the local environment, shows two different Li nuclei in significant proportion (assuming the third peak contributing 0.4% to be negligible). From both the results, we ascribe most of the lithium (87%) to occupy the tetrahedral 4d site and the remaining (12%) to probably occupy a position in the environment of the 12-coordinated vacant Sr site.

Interestingly, in our studies looking for the existence of the series $Li_{2x}Sr_{1-2x}M_{0.5-x}Nb_{0.5+x}O_3$ (for M = Fe and for various values of x), we also find indications of formation of other phases corresponding to the $n = 2$ and $n = 4$ members of RP phases. We are currently working on the exact composition, conditions of preparation, crystal growth, and the other properties of various members of this new series of oxides.

Conclusion

We have synthesized single crystals and bulk of $Li_4Sr_3Nb_{5.77}Fe_{0.23}O_{19.77}$ and $Li_4Sr_3Nb_6O_{20}$, for the first time. The analysis of the structure indicates that these compounds are related to the RP phases, with the 12-coordinated strontium sites being partially occupied. Our electron diffraction analyses also confirm that the compounds are RP-related $n = 3$ phases. Interestingly, the equilateral oxygen atoms forming the middle NbO_6 octahedral layer are found to occupy the 8j sites with half-occupancy. We could observe an ordering of these sites, resulting in a twisting of the NbO_6 octahedra and consequently a larger cell, from the electron diffraction of some of the crystallites. The conductivity behavior obtained from the impedance spectroscopy and the existence of two kinds of Li^+ ions shown by NMR analysis indicate the conduction path for the oxides is through vacant strontium sites, which accounts for the conductivity at elevated temperature in these phases. With indications for the formation of $n = 2$ and 4 members of Ruddlesden−Popper-related phases, the system Li−Sr−Nb−Fe−O seems to be a potential field for the investigation of various members of the Ruddlesden−Popper related phases.

Acknowledgment. We thank Dr. V. Maisonneuve for his help in collecting the single crystal X-ray diffraction data. One of us (N.S.P.B.) thanks the Région des Pays de la Loire for a postdoctoral fellowship and Ms. H. Duroy for her help in X-ray photographic analysis. Our sincere thanks are also to Mr. A. Barreau of Université de Nantes, Nantes, for his help in carrying out EDX analysis of the samples.

CM980736J

(26) Massiot, D.; Threle, H.; Germanus, A. *Bruker Rep.* **1994**, *43*, 140.